Progress In Electromagnetics Research Letters, Vol. 119, 99-105, 2024

PIER Letters

(Received 24 March 2024, Accepted 9 May 2024, Scheduled 14 May 2024)

Analysis of Fractal AMC Backed Gain Enhancement for Circular Spike Monopole Antenna

Rajesh Katragadda[1,*] and Palasetti Appala Nageswara Rao[2]

[1]*Department of ECE, AU Trans-Disciplinary Research HUB (A.U. TDR-HUB)*
Andhra University, Visakapatnam, Andhra Pradesh, India
[2]*Department of ECE, Gayatri Vidya Parishad College for Degree and PG Courses (A)*
Andhra University, Visakapatnam, Andhra Pradesh, India

ABSTRACT: This work provides the design, analysis, and performance optimization of an artificial magnetic conductor (AMC)-based wideband printed monopole antenna. The proposed antenna structure is constituted with CPW feeding, and an AMC layer has been added beneath the proposed antenna configuration to decrease back lobe radiation. By employing an AMC reflector, composed of periodic copper metallic Minkovski square fractal patches on a circular serrated antenna with an air gap separation of 8 mm, the proposed antenna has obtained a peak gain of 12.9 dBi, and wideband is also achieved by the antenna for wearable applications. The prototyped model of cotton fabric substrate material based measurement results with antenna measurement setup match the CST-tool simulation results, enabling the applicability in real time communication systems.

1. INTRODUCTION

Since wearables allow wireless communication between the wearable and its surroundings, they are becoming a growing trend for a variety of applications including consumer electronics, healthcare, fitness tracking, military, and entertainment. The use of wearable antennas is becoming increasingly popular in many fields, including healthcare. Despite initial efforts to design wearable antennas that could operate near human body, these antennas ultimately failed to meet expectations in terms of gain, front-back ratio, and radiation efficiency.

This was because depending on the antenna's design, the reflection coefficient (S_{11}) changed to one side of the resonance frequency. Antennas that may be worn by the user are essential in biological applications [1, 2] that include wireless connection with nearby equipment, a phenomenon called body-centric networks. Compact size and small bandwidth are the limitations for designing wearable antennas, and furthermore, wearable antennas must be designed to be long-lasting, practical, safe, usable, and convenient [3, 4]. The dielectric mediums that are utilized for flexible antenna design are felt, jeans, polyester, cotton, wool, polyester, silk, Cordura, Panama, etc. Moreover, regulatory agencies have determined that these antennas cause an increase in specific absorption rate (SAR) values, which in turn increases the possibility of tissue harm to the user [5]. With these considerations, it is crucial to design wearable antennas of the smallest possible size [6]. These issues are being actively investigated and addressed by researchers and antenna engineers. Numerous antenna topologies designed for application as textile antennas have been designed and reported. Such antenna topologies include monopoles [7], cavity-backed antennas [8], wearable antenna with substrate integrated waveguide technology [9], inverted-F antennas [10], and microstrip patch antennas [11]. Unfortunately, these antenna designs are not suitable for wearable technology because they are bulky, possess a small bandwidth, poor gain, and generate an enormous amount of back-lobe radiation, which raises the SAR value. To overcome these issues that wearable antennas encounter, a variety of techniques have been proposed [12–14]. However, these methods have some drawbacks.

When it comes to body centric communication, metamaterials (MMTs) have shown great promise to enhance the functionality of a wearable antenna. The AMC and electromagnetic bandgap (EBG) are two more alternative MMT designs that imitate perfect magnetic conductor (PMC) characteristics and suppress surface waves, respectively [15, 16]. To achieve design goals including gain, bandwidth, and efficiency, wearable antennas based on metamaterial structures are chosen and optimized. Several alternative metamaterial-based topologies have been presented for the use in wearable antennas that include fractal, patch, and planar spiral ones [17]. By examining the nature of metamaterial properties, we have proposed an AMC structure based on metamaterial nature, and the paper is organized as follows.

2. ANTENNA DESIGN ANALOGY

As illustrated in Fig. 1, the proposed antenna is designed on an FR4 substrate initially, and later a cotton substrate is chosen at the end based on its better performance. The antenna dimensions are presented in Table 1. From Fig. 2, it can be noted that the proposed structure resonates from 3.2 GHz to 10 GHz

* Corresponding author: Rajesh Katragadda (katragaddarajeshau@gmail.com).

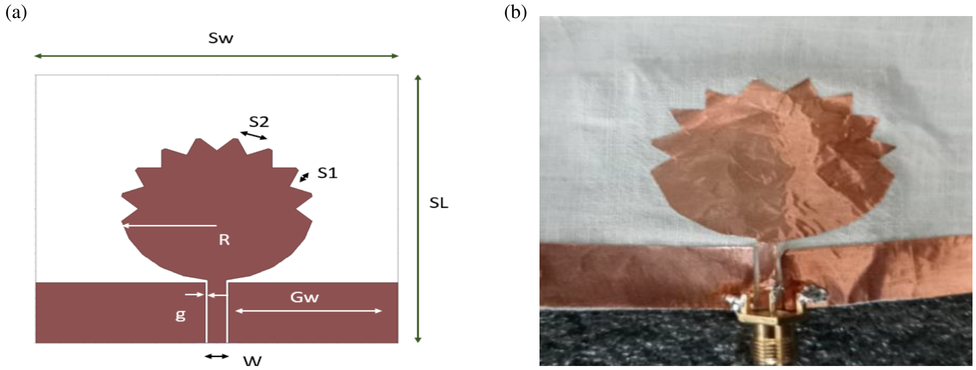

FIGURE 1. Circular serrated antenna representation using (a) simulation, (b) fabrication on a cotton material.

S_L	S_w	G_w	W	G	r	S_1	S_2
60.0	60.0	13.70	2.0	0.50	3.40	3.60	4.60

TABLE 1. Antenna modelling dimensions in mm.

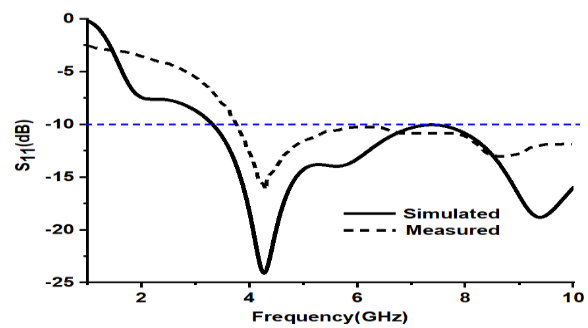

FIGURE 2. S_{11} response of the proposed circular serrated antenna.

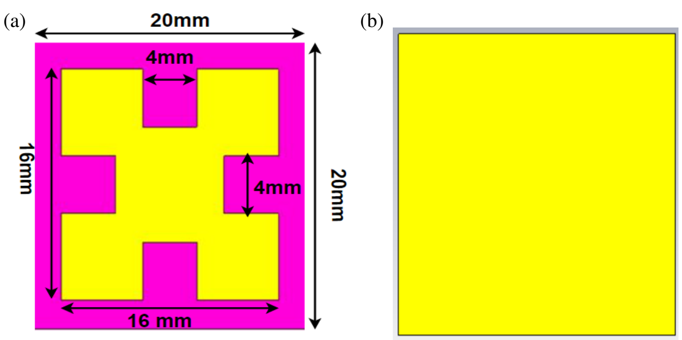

FIGURE 3. Unit cell of the proposed AMC, (a) front and (b) back sides.

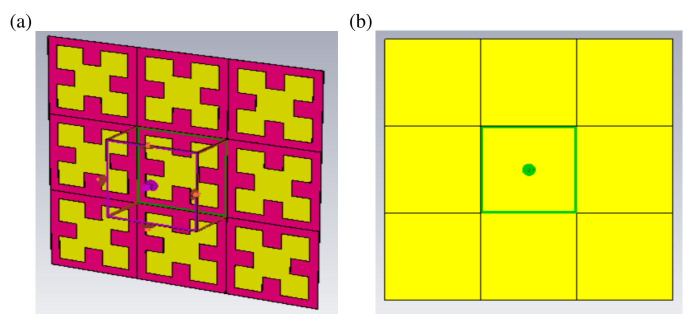

FIGURE 4. Simulation setup of the proposed unit cell, (a) front and (b) back views.

with minimum S_{11} magnitude of -24.23 dB using simulation and achieves S_{11} magnitude of -17.92 dB using measurement.

2.1. AMC Design Analogy

The proposed AMC (artificial magnetic conductor) surface is designed using a Minkovski fractal structure. As shown in Fig. 3, the proposed square fractal unit cell structure consists of three layers: copper for the bottom layer, jeans material to act as a dielectric medium, and a Minkovski square fractal typed patch as a radiating element. The unit cell size is $20 \times 20\,\text{mm}^2$, and the square patch size is $16 \times 16\,\text{mm}^2$, as indicated in Fig. 1. CSTMW studio is utilized for solving numerical calculations for the proposed design. In the simulation setup, the application of periodic boundary conditions in the X and Y axes, respectively, causes the electromagnetic wave impingement along the Z-axis, and as illustrated in Fig. 4, its S_{11} response is as shown in Fig. 5.

Metamaterial refers to something beyond naturally available material. From Fig. 6, it can be clearly noted that the proposed unit cell structure exhibits metamaterial properties within the operating frequency range and has the ability to change the EM wave characteristics. Only unit cell analysis will not give the complete performance of a metasurface design. So array analysis must be considered to assess the overall performance of a metasurface. Fig. 7 depicts different array sizes (2×2, 3×3 and 4×4) for unit cells. From Fig. 8, it is a fact that for any array size of the unit cell, the obtained S_{11} response is the same as S_{11} response of the proposed unit cell.

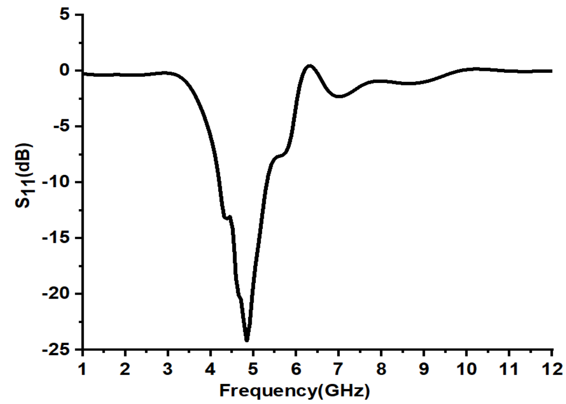

FIGURE 5. S_{11} response of the proposed unit cell design.

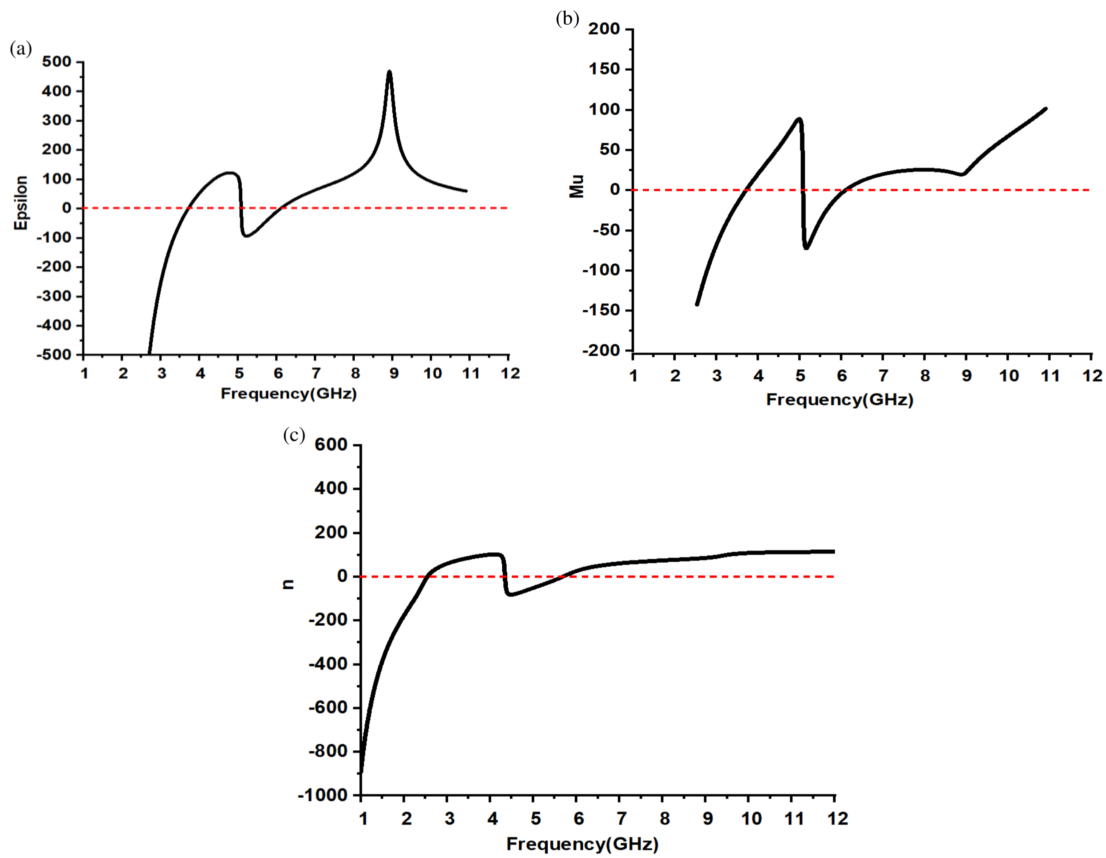

FIGURE 6. Metamaterial characteristics of the proposed unit cell, (a) ϵ, (b) μ and (c) n.

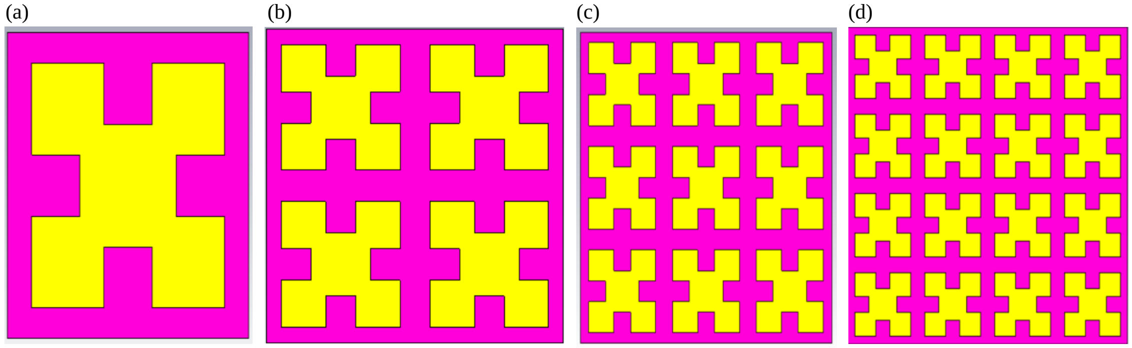

FIGURE 7. Different array sizes of the proposed unit cell design, (a) unit cell, (b) 2×2, (c) 3×3, (d) 4×4.

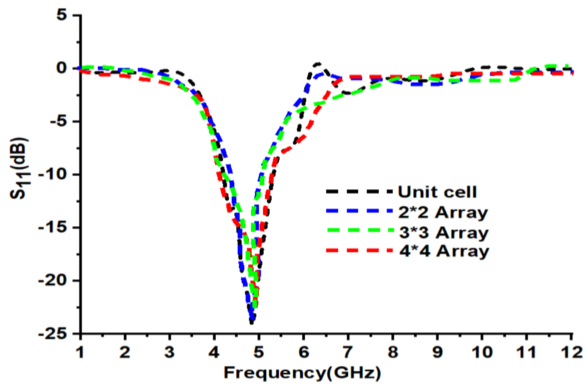

FIGURE 8. S_{11} response of the proposed unit cell with different array sizes.

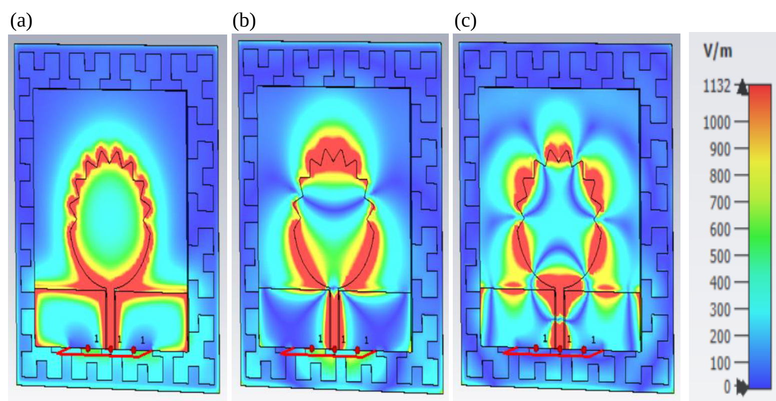

FIGURE 9. E-field distribution at (a) 6, (b) 7 and (c) 9.25 GHz frequencies.

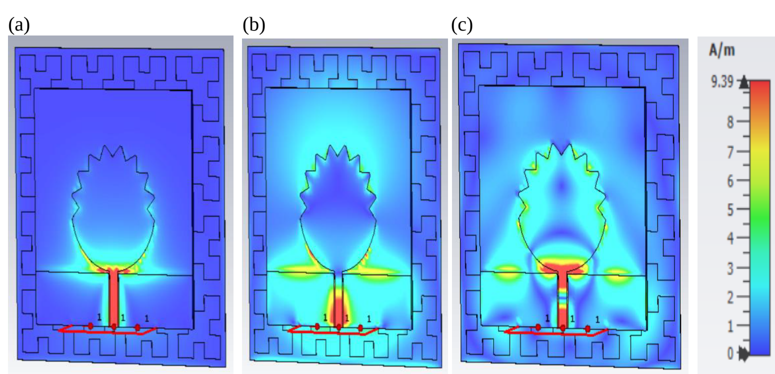

FIGURE 10. H-field distribution at (a) 6, (b) 7 and (c) 9.25 GHz frequencies.

From Fig. 9, it can be noted that at 6 GHz frequency a maximum amount of E-field is formed on serrated and circular shape. Similarly E-field is bifurcated into two parts on radiating patch of the proposed antenna, and a small amount of E-field can be observed on AMC radiating patch, and finally at 9.25 GHz frequency, the field is split into 4 parts.

From Fig. 10, it can be noted that at 6 GHz frequency a maximum amount of H-field is formed on serrated shape; maximum amount of H-field can be observed on semi-circle shape of the radiating patch; and a small amount of H-field can be observed on AMC. From Fig. 11, it is a fact that a maximum amount of current can be observed on feed line and semi-circle shape of the radiating patch.

3D radiation patterns at 6, 7, and 9.25 GHz frequencies are illustrated in Fig. 12, and from Fig. 12, it is a fact that a maximum peak gain (dBi) can be obtained at 7 GHz frequency, and a minimum peak gain (dBi) can be observed at 9.25 GHz frequency. The proposed AMC which is fabricated on a teflon material is shown in Fig. 13, and its measurement setup and placement of antenna with AMC is shown in Fig. 14. A foam material of 10 mm is placed between antenna and AMC. The obtained S_{11} response for the proposed antenna with an AMC is shown in Fig. 15. From Fig. 15, it can be noted that except from 7.5 GHz

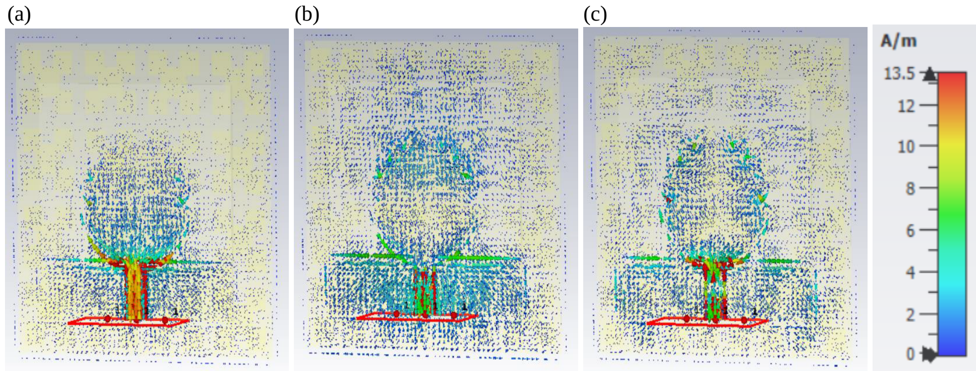

FIGURE 11. Surface current distributions at (a) 6, (b) 7 and (c) 9.25 GHz frequencies.

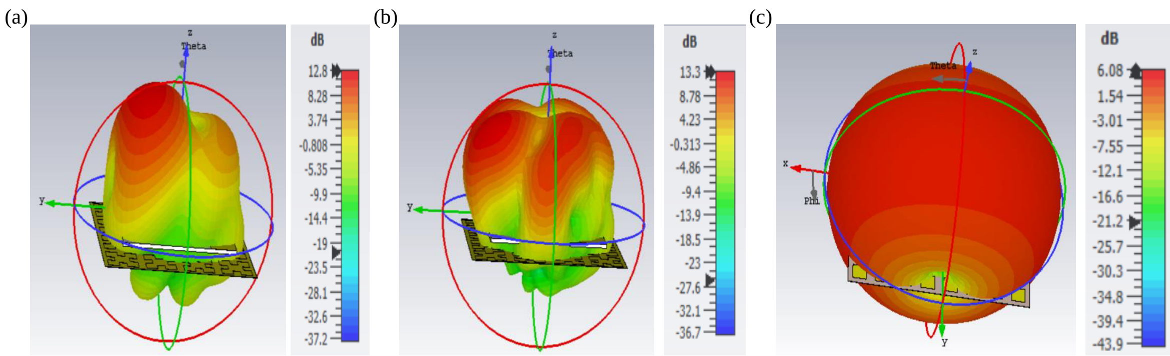

FIGURE 12. 3D-radiation patterns at (a) 6, (b) 7 and (c) 9.25 GHz frequencies.

FIGURE 13. Fabricated model of the proposed AMC on Teflon material.

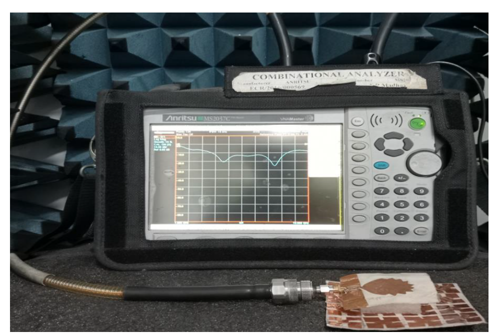

FIGURE 14. Measurement setup for the proposed antenna with proposed AMC.

TABLE 2. Comparision table of the proposed research work.

Ref.no	Antenna size (mm^2)	Shape of AMC	Dielectric substrate	Peak Gain (dBi)
[18]	60 ∗ 58	Square type patches	Lossy paper	5
[19]	45 ∗ 30	Joint cross	Kapton polyimide	-
[20]	30 ∗ 38.3	Square type patches	ROGERS4003	8.7
[21]	39 ∗ 32	Square type patches with square typed rings	Jeans	9.95
This work	60 ∗ 60	Square typed fractal patches	cotton	12.93

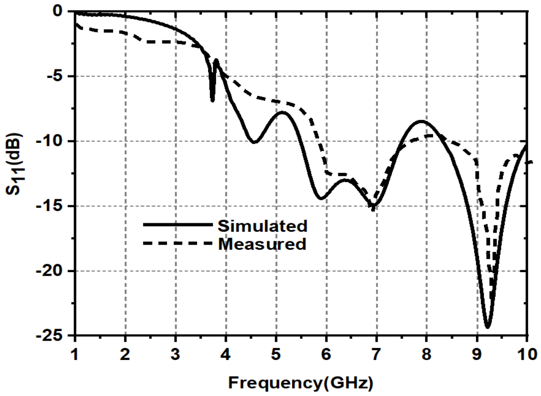

FIGURE 15. Simulated and measured S_{11} response for antenna with AMC.

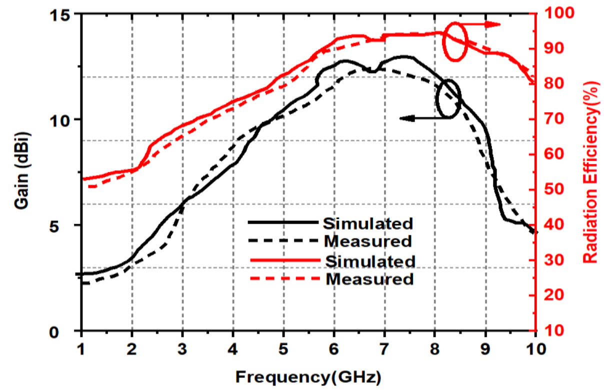

FIGURE 16. Gain and radiation efficiency response of the proposed antenna with an AMC.

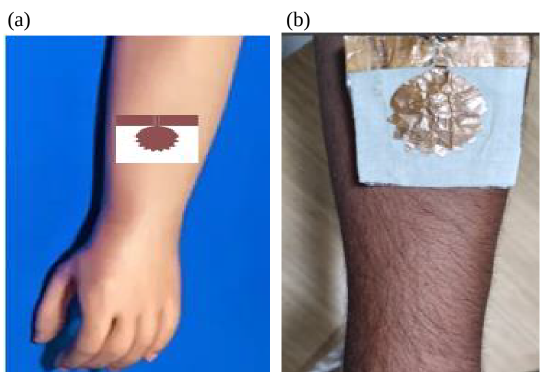

FIGURE 17. Antenna placed on human hand phantom model, (a) simulated phantom model, (b) human hand placement.

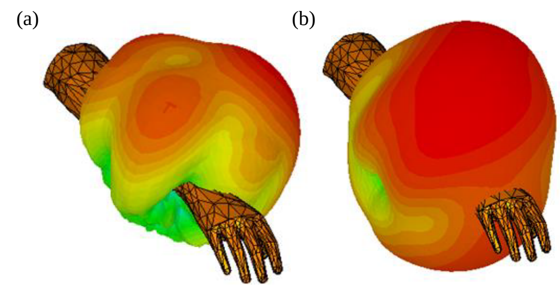

FIGURE 18. Simulated gain of antenna on human hand, (a) 6 GHz, (b) 7 GHz.

frequency to 8.23 GHz frequency S_{11} parameter resonates from 5.5 to 10 GHz frequency. The obtained gain and radiation efficiencies are shown in Fig. 16. From Fig. 14, it is a fact that the obtained gains at 6, 7, and 9.25 GHz frequencies are 12.62, 12.93, and 6.03 dBi, respectively. The radiation efficiencies for the proposed antenna with AMC are close to 90 percent. From Table 2, it can be clearly concluded that the proposed antenna produces a higher gain 12.93 dBi than existing literature.

The antenna is placed on human hand phantom model as shown in Fig. 17. The simulated model and the antenna placed on human hand in real environment are presented in Fig. 17(a) and Fig. 17(b), respectively. The antenna gain plots after placing antenna on human hand are presented in Figs. 18(a) and (b) for 6 GHz and 7 GHz, respectively. The gains of 8.2 dB and 8.5 dB are attained due to the presence of hand. The gain value is reduced by almost 4 dB due to the no presence of AMC.

3. CONCLUSION

This study analyses, discusses, and evaluates the design principles, fabrication, and measurement of a 6.7 GHz wideband antenna for microwave applications. The metamaterial properties of the proposed AMC structure have been clearly verified. The E and H-field distributions for the proposed antenna with an AMC layer have been verified. In addition to broadband bandwidth, the proposed circular serrated antenna attained a peak gain of 12.9 dBi by placing an AMC layer below the circular serrated antenna. The proposed fabric substrate-based design can be used for conformal and wearable communication applications.

REFERENCES

[1] Wu, J.-F., C. Qiu, Y. Wang, R. Zhao, Z.-P. Cai, X.-G. Zhao, S.-S. He, F. Wang, Q. Wang, and J.-Q. Li, "Human limb motion detection with novel flexible capacitive angle sensor based on conductive textile," *Electronics*, Vol. 7, No. 9, 192, Sep. 2018.

[2] Faisal, F., Y. Amin, Y. Cho, and H. Yoo, "Compact and flexible novel wideband flower-shaped CPW-fed antennas for high data wireless applications," *IEEE Transactions on Antennas and Propagation*, Vol. 67, No. 6, 4184–4188, Jun. 2019.

[3] Ashyap, A. Y. I., Z. Z. Abidin, S. H. Dahlan, H. A. Majid, and G. Saleh, "Metamaterial inspired fabric antenna for wearable applications," *International Journal of RF and Microwave Computer-Aided Engineering*, Vol. 29, No. 3, e21640, Mar. 2019.

[4] Ali, U., S. Ullah, B. Kamal, L. Matekovits, and A. Altaf, "Design, analysis and applications of wearable antennas: A review," *IEEE Access*, Vol. 11, 14 458–14 486, 2023.

[5] Shakib, M. N., M. Moghavvemi, and W. N. L. B. W. Mahadi, "Design of a tri-band off-body antenna for WBAN communication," *IEEE Antennas and Wireless Propagation Letters*, Vol. 16,

210–213, 2017.

[6] Michel, A., R. Colella, G. A. Casula, P. Nepa, L. Catarinucci, G. Montisci, G. Mazzarella, and G. Manara, "Design considerations on the placement of a wearable UHF-RFID PIFA on a compact ground plane," *IEEE Transactions on Antennas and Propagation*, Vol. 66, No. 6, 3142–3147, Jun. 2018.

[7] Mousavi, P., B. Miners, and O. Basir, "Wideband L-shaped circular polarized monopole slot antenna," *IEEE Antennas and Wireless Propagation Letters*, Vol. 9, 822–825, 2010.

[8] Bohorquez, J. C., H. A. F. Pedraza, I. C. H. Pinzon, J. A. Castiblanco, N. Pena, and H. F. Guarnizo, "Planar substrate integrated waveguide cavity-backed antenna," *IEEE Antennas and Wireless Propagation Letters*, Vol. 8, 1139–1142, 2009.

[9] Moro, R., S. Agneessens, H. Rogier, and M. Bozzi, "Wearable textile antenna in substrate integrated waveguide technology," *Electronics Letters*, Vol. 48, No. 16, 985–987, Aug. 2012.

[10] Soh, P. J., G. A. E. Vandenbosch, S. L. Ooi, and N. H. M. Rais, "Design of a broadband all-textile slotted PIFA," *IEEE Transactions on Antennas and Propagation*, Vol. 60, No. 1, 379–384, Jan. 2012.

[11] Alomainy, A., Y. Hao, A. Owadally, C. G. Parini, Y. Nechayev, C. C. Constantinou, and P. S. Hall, "Statistical analysis and performance evaluation for on-body radio propagation with microstrip patch antennas," *IEEE Transactions on Antennas and Propagation*, Vol. 55, No. 1, 245–248, Jan. 2007.

[12] Hsiao, Y.-T., S.-C. Tuan, H.-T. Chou, and J.-S. Wang, "Applications of shielding techniques to enhance the antenna performance of mobile communications and reduce SAR induction in the human head," *Electromagnetics*, Vol. 25, No. 4, 343–361, May 2005.

[13] Chan, K. H., K. M. Chow, L. C. Fung, and S. W. Leung, "Effects of using conductive materials for SAR reduction in mobile phones," *Microwave and Optical Technology Letters*, Vol. 44, No. 2, 140–144, Jan. 2005.

[14] Haridim, M., "Use of rod reflectors for SAR reduction in human head," *IEEE Transactions on Electromagnetic Compatibility*, Vol. 58, No. 1, 40–46, Feb. 2016.

[15] Lai, J., J. Wang, W. Sun, R. Zhao, and H. Zeng, "A low profile artificial magnetic conductor based tri-band antenna for wearable applications," *Microwave and Optical Technology Letters*, Vol. 64, No. 1, 123–129, Jan. 2022.

[16] Ashyap, A. Y. I., S. H. B. Dahlan, Z. Z. Abidin, M. I. Abbasi, M. R. Kamarudin, H. A. Majid, M. H. Dahri, M. H. Jamaluddin, and A. Alomainy, "An overview of electromagnetic band-gap integrated wearable antennas," *IEEE Access*, Vol. 8, 7641–7658, 2020.

[17] Jairath, K., N. Singh, M. Shabaz, V. Jagota, and B. K. Singh, "Performance analysis of metamaterial-inspired structure loaded antennas for narrow range wireless communication," *Scientific Programming*, Vol. 2022, 1–17, May 2022.

[18] Cook, B. S. and A. Shamim, "Utilizing wideband AMC structures for high-gain inkjet-printed antennas on lossy paper substrate," *IEEE Antennas and Wireless Propagation Letters*, Vol. 12, 76–79, 2013.

[19] Raad, H. R., A. I. Abbosh, H. M. Al-Rizzo, and D. G. Rucker, "Flexible and compact AMC based antenna for telemedicine applications," *IEEE Transactions on Antennas and Propagation*, Vol. 61, No. 2, 524–531, 2012.

[20] Askari, H., N. Hussain, D. Choi, M. A. Sufian, A. Abbas, and N. Kim, "An AMC-based circularly polarized antenna for 5G sub-6 GHz communications," *Computers, Materials & Continua*, No. 12, 2997–3013, 2021.

[21] Mersani, A., L. Osman, and J.-M. Ribero, "Performance of dual-band AMC antenna for wireless local area network applications," *IET Microwaves, Antennas & Propagation*, Vol. 12, No. 6, 872–878, 2018.